Supplementary Methods

Subject populations

Sera and peripheral blood mononuclear cells (PBMCs) were obtained from normal donors or patients with CLL in accordance with the Declaration of Helsinki. All subjects gave written, informed consent for their blood products to be used for research under an institutional review board (IRB)-approved protocol. Blood was collected at The Ohio State University Wexner Medical Center (Columbus, OH). PBMCs were used fresh or stored in 1 ml aliquots at −140 °C and sera were stored in aliquots at −80 °C until used. Samples derived from two reported clinical trials[1,2] were utilized for pharmacodynamic studies.

Cell culture, drug treatments, and T cell polarization

Primary T-cells were isolated using RosetteSep untouched CD3 or CD4 selection, EasySep Naïve CD4+ T-cell enrichment kits (STEMCELL Technologies, Vancouver, BC, Canada) or magnetic separation (MACS Human CD8+ microbeads, Miltenyi, Auburn, CA) according to the manufacturer's protocol.

Cells were cultured *in vitro* at 37°C and 5% CO2 using RPMI1640/10% fetal calf serum. Cells were pre-treated for 30 minutes with ibrutinib, washed 2X, then stimulated with plate-bound anti-CD3 and soluble anti-CD28 (eBiosciences, San Diego, CA). Cells were allowed to gently rest on CD3 coated plates while incubating at 37˚C. Nuclear and cytoplasmic lysates (NEN-PER kit, Thermo, Rockford, IL) were collected after 45 minutes and whole cell lysates were collected at 2 hours.

Th1 and Th2 polarized primary CD4 T-cells were generated according to our previously published methodology[3]. In brief, T-cells were obtained from magnetically purified naïve human CD4 T cells[3]. Cells were stimulated weekly with plate-bound anti-CD3, soluble anti-CD28, and IL-2 (20 U/ml) in the presence of IL-12 (10 ng/ml) and anti-IL-4 (1:100) for Th1 or IL-4 (5 ng/ml) and anti-IL-12 (1:100).

Calcium flux analysis

Jurkat cells were stained with Fluo4-AM (Invitrogen) for 30 minutes at 37˚ in complete RPMI medium. Simultaneously cells were incubated with the indicated concentration of ibrutinib or vehicle (DMSO) or BAPTA-AM (Invitrogen) intracellular calcium chelator. Afterwards, cells were washed twice and resuspended in phenol-red free RPMI. Fluo4 fluorescence was measured using a plate reader at 535nm. Baseline activation was measured for 300 seconds followed by the addition of functional grade anti-CD3 (eBiosciences) and activation was immediately measured for an additional 500 seconds. Baseline fluorescence was subtracted as was BAPTA negative control fluorescence. Area under the curve (AUC) measurements were calculated using the trapezoidal rule as previously published[4].

Reverse transcriptase-PCR (RT-PCR)

Total RNA was prepared from pelleted cells (RNeasy mini columns and RNAse free DNAse, Qiagen, Valencia, CA). RT-PCR and qRT-PCR reactions were conducted using the Qiagen one-step RT-PCR kit (Qiagen) or the iScript SYBR green RT-PCR kit (BioRad, Hercules, CA) with transcript-specific primers (mITK: 5’ GGTCATCAAGGTGTCCGACT, 3’ TCGTATGGGATTTTGCCTTC) (mBTK:

5’AAAGGTTCCCGTACCCATTC, 3’CCCATAGCATTCTTGGCTGT) (mGAPDH: 5’CTCATGACCACAGTCCATGC, 3’CACATTGGGGGTAGGAACAC) (hGAPDH: 5’AGAAGGCTGGGGCTCATTTG, 3’AGGGGCCATCCACAGTCTTC) (hRLK: GTACGGAGGCTGCCATAAAA, 3’CAGCTGTGGCTGGTAAACAA) and 200 ng of total RNA. RT-PCR amplification reactions were resolved on 2% agarose gels and the size of the amplified transcript confirmed by comparison with a standard DNA ladder (GelPilot 1 Kb Plus Ladder, Qiagen). qRT-PCR experiments were analyzed using the MyiQ software package. After confirming a single melt curve peak CT values for GAPDH were compared to CT values for the transcript of interest using the Pfaffl method[5].

Flow cytometry and cytokine bead array (CBA)

Flow cytometric analysis was performed using fluorochrome-labeled monoclonal antibodies (mAbs; anti-CD3, -CD4, -CD5, -CD8, -CD19, -CD62L, -CD45RA, -IL-4, -IFNγ, Annexin V, PI, Becton Dickinson, San Jose, CA). Intracellular staining was conducted according the appropriate manufacturer protocol (Becton Dickinson). For intracellular staining of IL-4 and IFNγ, PMA and ionomycin stimulation was utilized. For phosphoflow analysis of PLCγ1, cells were fixed with 4% paraformaldehyde/PBS after surface staining and permeablized in cold 90% methanol. Intracellular staining used anti-pPLCγ1-Tyr783 (Cell Signaling Technologies, cat#2821S) followed by anti-rabbit Alexa488 (Invitrogen, cat#A11008). CBA (Becton Dickinson) was conducted according to the manufacturers published protocol using cellular supernatant from three replicate experiments or mouse plasma. CFSE and PKH26-based cell proliferation assays were performed as previously described[3,6]. Flow cytometric data was analyzed with FlowJo

or Kaluza software (Tree Star, Ashland, OR) (Beckman Coulter, Indianapolis, IN) on a minimum of 30,000 collected events.

Flow cytometry-based tetramer staining was conducted on 50 µl of whole blood for 1 hour on ice in PBS (+5% FBS, +0.02% NaN_3) with anti-CD4, CD8, CD19 (Becton Dickinson) and 2 µg/ml Alexa647-H-2K(b) SIINFEKL tetramer (NIH Tetramer Facility). Afterwards, erythrocytes were lysed according to the manufacturer's protocol (eBiosciences) and samples were washed once prior to analysis. Gates for tetramer positive CD8 T-cells were verified using the baseline samples obtained 7 days prior to *Listeria* infection and confirmed using FMO controls.

Ibrutinib probe assay

To determine percent ITK occupancy in patients treated with ibrutinib, PBMC were lysed by freeze-thawing 4 times. After the final thaw, cells were centrifuged at 16,000g for 10 min at 4C to pellet insoluble material. Protease inhibitors were added to the protein lysates, and the protein lysates were labeled with a biotinylated derivative of ibrutinib for 1hr at RT and added to a Streptavidin coated plate (MSD, cat #L15SA-2) that was blocked for 1hr with blocking solution. Afterwards, the plates were washed 3x and incubated with mouse anti-ITK (BD#550503) for 1hr. After washing 3X plates were incubated for 1hr with SULFO-TAG conjugated anti-mouse antibody (MSD, cat#R32AC-5), washed, and read on a SI2400 for 3 min according to manufacturer's instructions. Percent occupancy was calculated based upon available probe binding sites as compared to an ibrutinib untreated control sample.

Immunoblot analysis

Experiments were conducted using conventional methodology previously described[7]. Blotting was conducted using pZAP70 #2717, ZAP70 #3165, pLAT #3584, LAT #9166, pLCK #2751, LCK #2787, pSTAT1 #9177S, STAT1 #9176, NFAT1 #4389S, pITK #3531S, ITK #2380S, JUNB #3746S, pIKBα #9246L, pSTAT6 #9361S, and STAT6 #9362S (Cell Signaling Technologies, Danvers, MA), T-bet #14-5825-82 (eBiosciences), IkBα #sc-371, BRG1 #sc-17796, TCL1 #sc-32331, and β-Actin #sc-1616 (Santa Cruz Biotechnology, Santa Cruz, CA) specific antibodies. Densitometry analysis was conducted using Image J analysis software (NIH). Raw density was normalized to the intensity of vehicle treated stimulated cells.

Confocal immunofluoresence microscopy of fixed cells

Cells were centrifugally concentrated on microscope slides using a Cytospin3 (Thermo) centrifuge and stained as previously described[6]. Cells were then fixed in PBS/2% paraformaldehyde. Slides were incubated in blocking solution (4% bovine serum albumin in PBS) and stained for NFAT1 (Cell Signaling, Boston, MA) by incubating with the primary antibodies overnight at 4˚C, followed by incubation with fluorescent secondary antibody Alexa fluor 488 (Invitrogen, Carlsbad, CA). Nuclei were stained blue with DAPI (Vector Laboratories, Burlingame, CA). Images were taken using a 60x objective and 4x digital zoom with Olympus Fluoview 1000 Laser Scanning Confocal microscope at the Ohio State University Campus Microscopy and Imaging Facility.

Mouse Models

C57BL/6 mice and EμTCL1 transgenic (Tg) mice on a C57BL/6 background were housed in microisolator cages under controlled temperature and humidity. All animal

procedures were performed in accordance with Federal and Institutional Animal Care and Use Committee requirements. For longitudinal analysis of Th1/Th2 skewing, 4 week old EμTCL1 transgenic animals were given drinking water containing sterile control vehicle (1% hydroxypropyl-b-cyclodextrin; HP-β-CD) or ibrutinib in 1% HP-β-CD, at 0.16 mg/mL. The volume of water consumed and the body weight of mice were recorded. On average mice took 0 or 25 mg/kg/d ibrutinib for a total of 8 months. For leukemia/listeriosis studies, adoptive transfer of $1x10^7$ freshly isolated splenocytes from EμTCL1 animals was performed. In this model, mice usually succumb from tumor in 8-10 weeks. One week after injection of leukemia cells, mice were given drinking water containing sterile control vehicle (1% HP-β-CD) or ibrutinib in 1% HP-β-CD, at 0.16 mg/mL. On average, mice took 25 mg/kg/d ibrutinib for a total of 16 days. 14 days after engraftment mice were challenged with a sub-lethal intravenous dose (5000CFU) of recombinant *Listeria monocytogenes* (rLM-OVA, a kind gift from Dr. Michael J. Bevan, University of Washington, Seattle, WA). During treatment, blood was drawn regularly to track disease progression. Individual mice were euthanized and assessed for *Listeria* growing in the liver compartment at days 2, 8, and 13.

Two days prior to infection, 6-8 week old BALB/c mice (Jackson labs, Bar Harbor, ME) were randomly assigned to vehicle or ibrutinib treatment groups. Ibrutinib was administered via drinking water as previously described for *L. monocytogenes* experiments. At day zero $2x10^6$ stationary phase *Leishmania major* promastigotes were injected into the rear left footpad and lesions were monitored weekly for development of cutaneous leishmaniasis. Popliteal lymph nodes were collected for Interim analysis of

T-cell cytokines at week 9. Footpad lesions were mashed and parasite load calculations were determined using standard methodology[8].

Enzyme linked immunoabsorbent assay (ELISA)

Submandibular blood was collected and plasma was centrifugally separated. An ELISA assay was performed for each IgG subisotype using a clonotyping system (B6/C57J-AP-5300-04B, Southern Biotech, Birmingham, AL) according to manufacturer's instructions on EIA/RIA high binding 96 well plates (Costar 3590, Corning, NY). Plasma dilutions were made in 1XBBS as follows: IgG1-1:10,000, IgG2c-1:10,000. A standard curve was utilized for each isotype on each individual plate (B6/C57J Mouse Immunoglobulin Panel-5300-01B, Southern Biotech) and the sample triplicate averages were read from the curve at 405nm using a spectrophotometer (Labsystem Multiskan MCC/340, Fisher Scientific). IL4, IL10, IL13, and IFNγ analysis of popliteal lymph node cells derived from L. major infected mice was conducted as previously described[9]. In brief, cells were stimulated with soluble *L. major* antigen for 72hr. Culture supernatants were collected for ELISA based analysis.

Statistics

Unless otherwise noted, a two-tailed student's T-test was used for normal data at equal variance. Significance was considered for $p<0.05$. Comparisons of IL4 and IFNγ expression in CD4 T-cells were performed using mixed effects models to allow for dependencies among observations from the same patient. From the model, estimated differences in expression at each of the five dose levels were estimated, with 95% CI, with an adjusted significance level of $\alpha=0.01$. Similarly, for *Listeria*/leukemia mouse

models a mixed effects model was applied to log-transformed data, and the interaction between condition and time was assessed. From the model, the change in percentage tetramer positive from baseline (day -7) to the peak (day +8) between the ibrutinib and vehicle groups, as well as healthy *Listeria* and control groups, were estimated with 95% CI. All analyses were performed using SAS/STAT software, v9.2 (SAS Institute Inc., Cary, NC).

Supplementary References

1. Jaglowski SM JJ, Flynn JM, Andritsos LA, Maddocks KJ, Blum KA, Grever MR, Geyer SM, Woyach JA, Johnson AJ, Heerema NA, Molnar E, Stefanos M, Devlin S, Navarro T, James DF, Lowe AM, Hedrick E, Byrd JC. A phase Ib/II study evaluating activity and tolerability of BTK inhibitor PCI-32765 and ofatumumab in patients with chronic lymphocytic leukemia/small lymphocytic lymphoma (CLL/SLL) and related diseases. *J Clin Oncol* 2012;30((suppl; abstr 6508)).
2. Advani RH, Buggy JJ, Sharman JP, et al. Bruton tyrosine kinase inhibitor ibrutinib (PCI-32765) has significant activity in patients with relapsed/refractory B-cell malignancies. *J Clin Oncol*;31(1):88-94.
3. Dubovsky JA, Powers JJ, Gao Y, Mariusso LF, Sotomayor EM, Pinilla-Ibarz JA. Epigenetic repolarization of T lymphocytes from chronic lymphocytic leukemia patients using 5-aza-2'-deoxycytidine. *Leuk Res*. 2011;35(9):1193-1199.
4. Manjarrez-Orduno N, Marasco E, Chung SA, et al. CSK regulatory polymorphism is associated with systemic lupus erythematosus and influences B-cell signaling and activation. *Nat Genet*. 2012;44(11):1227-1230.
5. Pfaffl MW. A new mathematical model for relative quantification in real-time RT-PCR. *Nucleic Acids Res*. 2001;29(9):e45.
6. Dubovsky JA, Wang D, Powers JJ, et al. Restoring the functional immunogenicity of chronic lymphocytic leukemia using epigenetic modifiers. *Leuk Res*. 2011;35(3):394-404.
7. Lapalombella R, Yeh YY, Wang L, et al. Tetraspanin CD37 Directly Mediates Transduction of Survival and Apoptotic Signals. *Cancer Cell*. 2012;21(5):694-708.
8. Fowell DJ, Shinkai K, Liao XC, et al. Impaired NFATc translocation and failure of Th2 development in Itk-deficient CD4+ T cells. *Immunity*. 1999;11(4):399-409.
9. Cummings HE, Barbi J, Reville P, et al. Critical role for phosphoinositide 3-kinase gamma in parasite invasion and disease progression of cutaneous leishmaniasis. *Proc Natl Acad Sci U S A*. 2012;109(4):1251-1256.

Supplementary Figure Legends

Supplementary Figure 1: Occupancy of ITK by ibrutinib after macromolecular complex disassociation. Jurkat cell lysates were directly treated with ibrutinib-probe at the indicated concentration and then assayed for covalent binding of ITK. Percent occupancy of total cellular ITK is depicted.

Supplementary Figure 2: ITK and downstream T-cell signaling pathways are disrupted by ibrutinib in Jurkat T-cells. (a) Immunoblot analysis of ibrutinib pretreated, anti-CD3/anti-CD28 stimulated (or unstimulated), Jurkat whole cell lysates. Blot probed for pITK-Y_{180}, Total ITK, pIkBα-$S_{32/36}$, Total IkBα, and Actin. (b) Immunoblot analysis of ibrutinib pretreated, anti-CD3/anti-CD28 stimulated (or unstimulated), Jurkat whole cell lysates. Blot probed for pSTAT6-Y_{641}, Total STAT6, pIkBα-S32/36, Total IkBα, JunB, and Actin. (c) Immunoblot analysis of ibrutinib pretreated, anti-CD3/anti-CD28 stimulated (or unstimulated), Jurkat cytoplasmic and nuclear lysates. Blots probed for NFAT (and activated hyper-dephosphorlyated NFAT), Brg1 (nuclear loading control), and Actin (cytoplasmic loading control).

Supplementary Figure 3: Immunoblot analysis of JAK3 inhibitory effects of ibrutinib in primary T-cells. Primary T cells were isolated using RosetteSep Human T cell enrichment kit, and treated with either Ibrutinib or CP-690, 550 (JAK1/3 inhibitor) at 0, 0.01, 0.1 or 1 μM for 1 hr and stimulated with 100 nM rhIL-2 for 10 minutes. Blots were probed for STAT5 (Cell Signaling 9358), pSTAT5 (Cell signaling 9359) and JAK3 (Cell signaling 3775).

Supplementary Figure 4: Proximal T-cell signaling is unaffected by ibrutinib in Jurkat T-cells. Immunoblot analysis of ibrutinib pretreated, anti-CD3/anti-CD28 stimulated (or unstimulated), Jurkat whole cell lysates. Blot probed for pZAP70-Y_{319}, Total ZAP70, pLAT-Y_{191}, Total LAT, pLCK-Y_{505}, Total LCK, pIkBα-$S_{32/36}$, Total IkBα, and Actin.

Supplementary Figure 5: Overall proliferative capacity of a mixed population of CD4 T-cells is maintained as is recall response after ibrutinib treatment. Top panel: $40E^6$ CFSE stained, freshly isolated, ibrutinib pretreated, and anti-CD3/anti-CD28 stimulated (or unstimulated) CD4+ cells from a healthy donor were assayed by flow cytometry after 7 days of *in vitro* culture. Durring that 7 days the cells had been stimulated by placing them on anti-CD3 coated plates and adding soluble anti-CD28. Bottom panel: half of the cells from the first week were re-stained with PKH26 and restimulated for an additional 7 days of *in vitro* culture using identical methodology. Flow cytometric analysis was conducted at the end of each week. Gated cells represent at least 1 cellular division. Each flow experiment contained a live/dead exclusion dye to isolate live cells for analysis.

Supplementary Figure 6: Flow cytometry analysis of naïve, terminal, central, and effector memory CD4+ T-cells before and after ibrutinib treatment. Flow cytometric analysis of naïve (N)(CD62L+CD45RA+), central memory (CM)(CD62L+CD45RA-), effector memory (EM)(CD62L-CD45RA-), and terminal memory ™(CD62L-CD45RA+) CD4+ selected T-cells isolated from a healthy donor. Cells were pretreated with the

indicated concentration of ibrutinib and stimulated (or unstimulated) with anti-CD3/anti-CD28 for 24 hours prior to analysis. Percentages are represented in each quadrant and each row represents a different healthy donor of varying age (between 30 and 56 years of age).

Supplementary Figure 7: Gating strategy for pPLCγ-Tyr783 analysis in CD3+CD4+ cells. A minimum of 400,000 cellular events were collected and gated on forward and side scatter to isolate lymphocytes. Size selected cells were subgated using a fixable live dead marker and live cells were gated on CD3 and CD4 to isolate double positive cells. Live CD3+CD4+ were gated on pPLCγ1-Tyr783 and relative positive and negative gates were generated based upon unstimulated and stimulated control samples.

Supplementary Figure 8: *In vitro* kinase data from ibrutinib, alternate BTK inhibitor, and PCI-45292. *In vitro* kinase assay IC_{50} inhibition of ITK and BTK for ibrutinib, Alternate BTK inhibitor, and PCI-45292.

Supplementary Figure 9: ITK irreversibly bound by the alternate BTK inhibitor as compared to ibrutinib in a Jurkat cellular assay. A molecular probe assay was used to calculate the percent occupancy of total ITK in Jurkat whole cell lysates irreversibly bound by ibrutinib (dark bars) or Alt. BTK inhibitor (open bars). Error bars, s.e.m.

Supplementary Figure 10: Chemical structure of an alternate BTK inhibitor.

Supplementary Figure 11: Immunoblot analysis of constitutive downstream BTK signaling in leukemic B-cells treated *in vitro* with three irreversible BTK inhibitors. Immunoblot analysis of whole cell lysates from freshly isolated 1μM ibrutinib, PCI-45292, Alt. BTK inhibitor, or vehicle (DMSO) treated primary CD19+ B-cells from a CLL donor. Blot was probed for pERK, Total ERK, and Actin.

Supplementary Figure 12: ITK binding probe assay conducted on Jurkat lysates pretreated with ibrutinib or PCI-45292. Fluorescent probe assay was used to calculate the percent occupancy of total ITK in Jurkat whole cell lysates irreversibly bound by ibrutinib (dark bars) or PCI-45292 (open bars). Error bars, s.e.m.

Supplementary Figure 13: ITK specific downstream signaling is attenuated by ibrutinib but not a structurally similar ITK non-targeting BTK inhibitor. Immunoblot analysis of nuclear and whole cell extracts from ibrutinib or PCI-45292 pretreated, freshly purified healthy donor primary CD4+ cells stimulated with anti-CD3/anti-CD28. Nuclear extracts were probed for NFAT1 and Brg1; whole cell extracts were probed for pSTAT1-Y701, Total STAT1, JunB, and Actin.

Supplementary Figure 14: ITK-C44A is expressed at the mRNA level in Jurkat cells containing the mutant construct. Sanger sequencing reaction chromatograms conducted on reverse transcriptase PCR amplified mRNA from Jurkat-ITKC_{442}A, Jurkat-

ITKwt, and Jurkat parental cell lines. Highlighted base pairs are the first two nucleotides in ITK codon 442 which code for a wt-Cys (TGC) or a mutant-Ala (GCC).

Supplementary Figure 15: T-cell receptor induced calcium flux is inhibited by ibrutinib and rescued by expression of ITK-C442A. Fluo4-AM calcium release analysis of Jurkat-ITK and Jurkat-ITKC442A cell lines after pretreatment with ibrutinib or DMSO and stimulation with anti-CD3. Each average represents four replicate experiments. Error bars s.e.m.

Supplementary Figure 16: RLK is not expressed at the mRNA level in Jurkat cells; however stable transduction of RLK yields Jurkat cells which express high levels of the kinase. Average qRT-PCR cycle of transmittance (Ct) values are depicted for GAPDH (control gene) and RLK in the stable clones of Jurkat parental, Jurkat-EV (Empty Vector), and Jurkat-RLK.

Supplementary Figure 17: T-cell receptor induced calcium flux is inhibited by ibrutinib and rescued by expression of RLK. Fluo4-AM calcium release analysis of Jurkat-EV (empty vector) and Jurkat-RLK cell lines after pretreatment with ibrutinib or DMSO and stimulation with anti-CD3. Each average represents four replicate experiments. Error bars s.e.m.

Supplementary Figure 18: Ibrutinib selectively inhibits IL4 producing CD4 T-cells obtained from healthy donor peripheral blood. Normalized intracellular staining

analysis of IL4 (open bars) and IFNγ (closed bars) in healthy donor CD4+ cells pretreated with ibrutinib and stimulated with anti-CD3/anti-CD28 (n=3). Error bars, s.e.m.

Supplementary Figure 19: B and CLL cell cytokine mRNA analysis reveals no ibrutinib-induced modulation of IL10, IL13, IL4, or IFNγ. CD19+ B-cells and CLL cells were isolated from peripheral blood at pre-dose and after 28 days on ibrutinib. Transcript-specific qRT-PCR analysis of IL10, IL13, IL4, and IFNγ mRNA levels were compared to GAPDH and subsequently to day 28 levels using the Pfaffl fold-change calculation.

Supplementary Figure 20: T-cell activation in ibrutinib treated mice phenocopies that of Itk-/- mice. Peripherial blood was obtained from 7-day ibrutinib or vehicle treated wild type (C57Bl/6) or Itk-/- mice. Anti-mouse CD3-biotin or a biotin conjugated isotype control antibody was added to 100µl aliquots of whole blood followed by streptavidin crosslinker (100ug/ml). Blood samples were incubated at 37˚ for 24 hours and activated CD4+CD45+CD14- T-cells were examined for upregulation of CD69 as compared to isotype.

Supplementary Figure 21: Ibrutinib does not directly alter the growth of leishmainia major parasites. *Leishmania major* parasites were treated with Ibrutinib (1uM concentration) for 24 hours before viability assessment by flow cytometry using propidium iodide staining. Untreated parasites were used as live cell control. Saponin

(100ug/ml) from Q. saponaria (Sigma-Aldrich) treatment of parasites for 30 minutes was used as permeabilized cell control.

Supplementary Figure 22: Gating strategy for OVA-Tetramer positive CD8 T-cells. (1) FS/SS gate for T and B lymphocytes. Backgating verified this gate included all CD19/CD4/CD8 positive events. (2) Gated on singlet events using FS-Peak vs. FS-Area plot. (3) Excluded CD19+ B-cells (4) Gated on CD4+ and CD8+ T-cells (5) Refined gate on CD8+ T-cells for tetramer analysis. The gate for tetramer positive CD8 T-cells was generating on an individual basis using the baseline tetramer staining 7 days prior to Listeria injection. The tetramer positive gate was set such that less than 0.04% CD8+ events would appear tetramer positive at day -7.

Supplementary Figure 23: Ibrutinib enhances the ability of leukemic mice to achieve sterilizing immunity of Listeria within the liver. Listeria m. cultures derived from mouse livers diluted 1:3 (grams : milliliters) at interim analysis points on day 2 (top row) and day 8 (bottom row) post infection. Colony forming units (CFU) are displayed as calculated from each plate. A 1:1000 dilution of Listeria m. inoculum confirms the viability of pre-injected Listeria m.

Supplementary Figure 24: Ibrutinib does not directly alter the growth or colony formation of Listeria monocytogenes bacteria. Growth kinetics of Listeria was assessed by optical density (O.D.600) after 4 hours of in vitro culture shaking at 37˚C. Bacterial cultures were continuously treated with 1μM ibrutinib or DMSO as indicated

(left panel). Colony formation was assessed for each culture using a standard dilution series (right panel).

Supplementary Figure 25: Ibrutinib does not alter the kinetics of recall responses in mice receiving a second infection of Listeria. Timecourse analysis of OVA-MHC I tetramer positive peripheral CD8 T-cells from leukemia/listeriosis mouse rechallenge (days 14-27). 5000CFU of OVA expressing-Listeria m. was injected at day 14. No statistically significant difference was observed between Ibrutinib, Vehicle, or Healthy groups at any analysis point. Error bars, s.e.m.

Supplementary Figure 26: Gating strategy for isolation of memory CD4 and CD8 lymphocytes from spleen isolates. A minimum of 200,000 cellular events were collected and gated on forward and side scatter to isolate lymphocytes. Size selected cells were subgated using a fixable live dead marker and live cells were gated on CD8 and CD4 to isolate individual T-cell subsets. Live CD4+ or CD8+ were gated on CD62L and relative positive and negative gates were generated based upon isotype stained controls.

Supplementary Figure 1

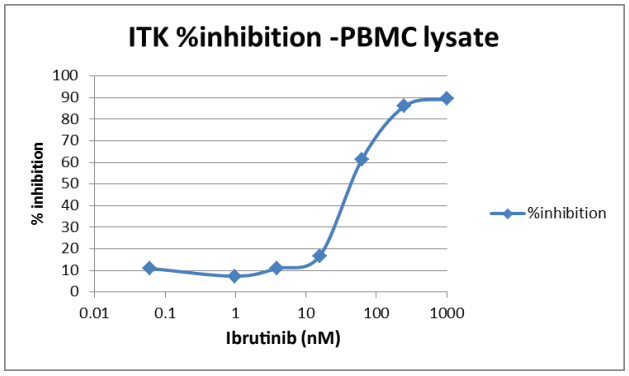

Supplementary Figure 2

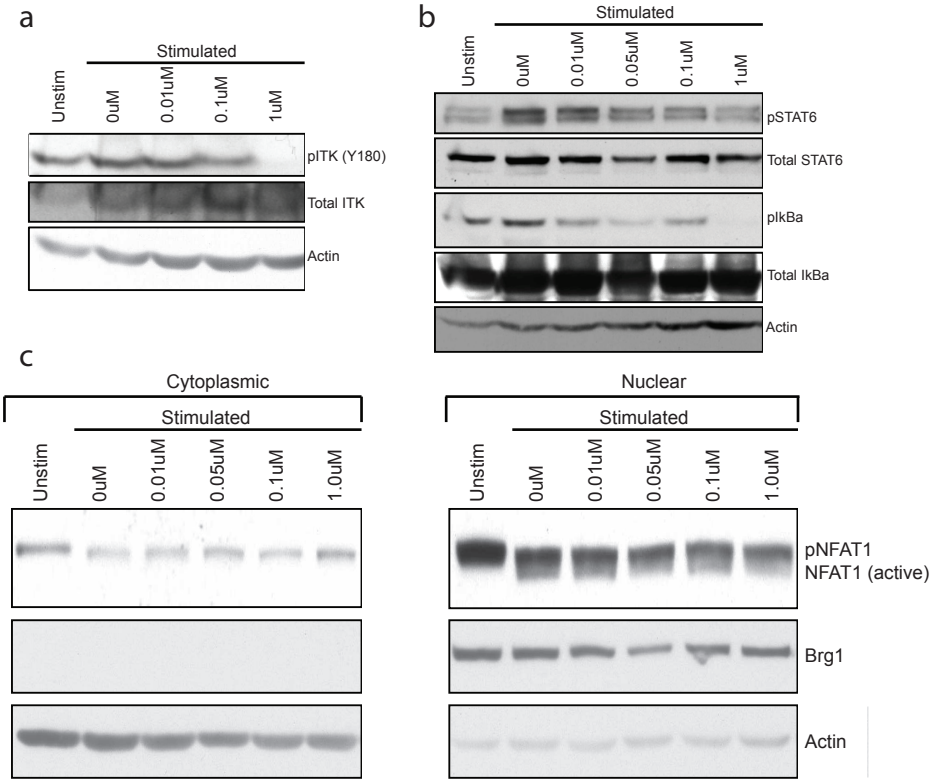

Supplementary Figure 3

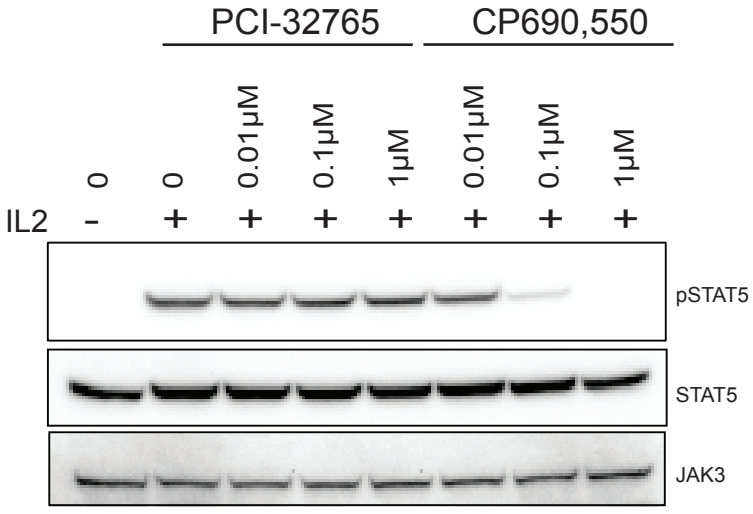

Supplementary Figure 4

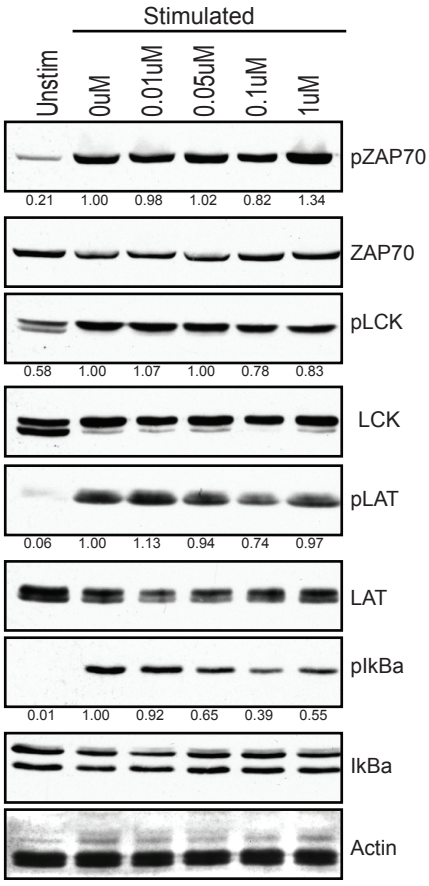

Supplementary Figure 5

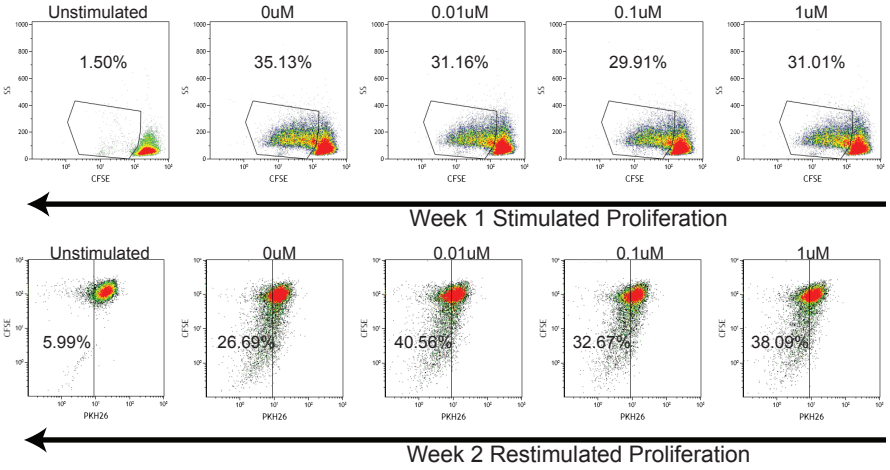

Supplementary Figure 6

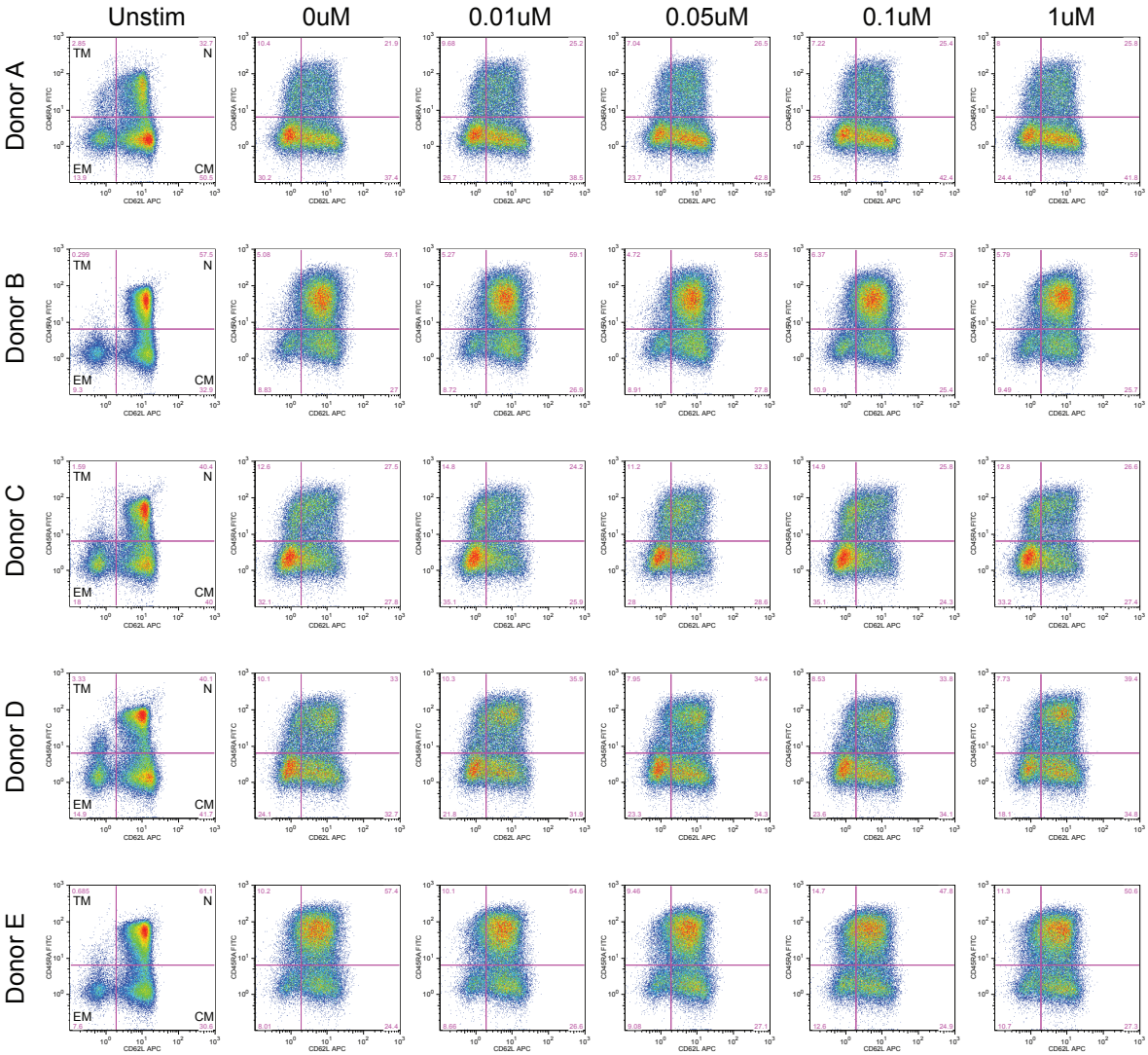

Supplementary Figure 7

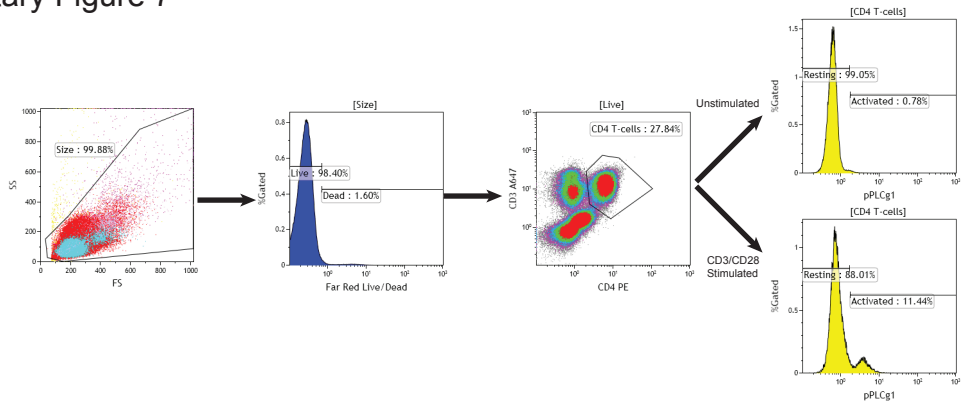

Supplementary Figure 8

Tyrosine Kinase	Ibrutinib IC_{50} (nM)	AVL-292 IC_{50} (nM)	PCI-45292 IC_{50} (nM)
ITK	2.2	22.5	139
BTK	0.1	1.8	0.78

Supplementary Figure 9

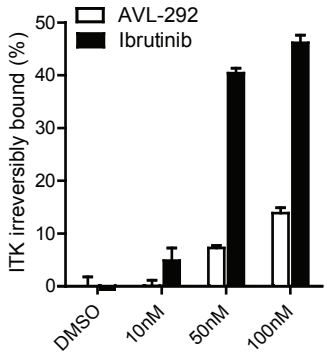

Supplementary Figure 10

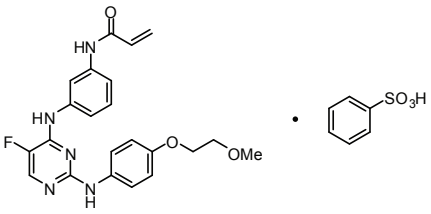

AVL-292

Chemical Formula: $C_{22}H_{22}FN_5O_3$
Exact Mass: 423.17
Molecular Weight: 423.44
Formula Weight: 581.62

Supplementary Figure 11

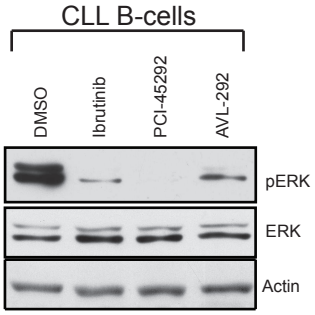

Supplementary Figure 12

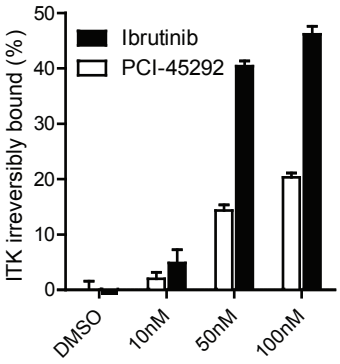

Supplementary Figure 13

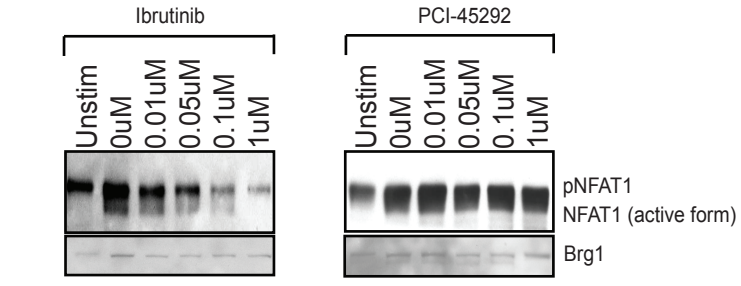

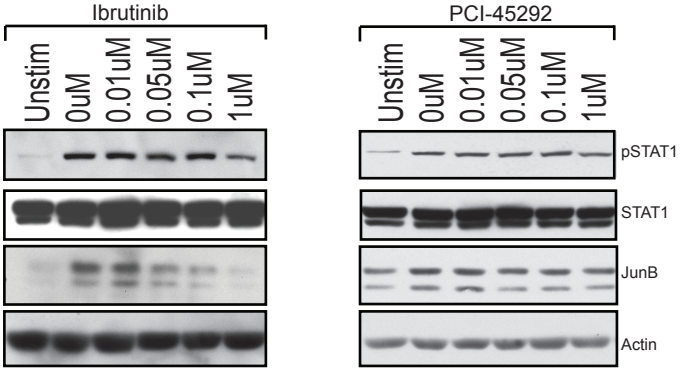

Supplementary Figure 14

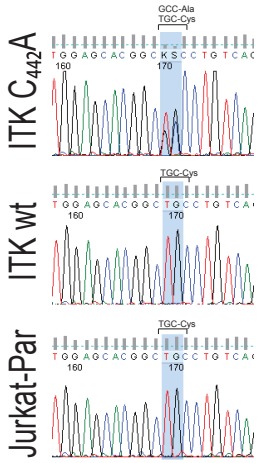

Supplementary Figure 15

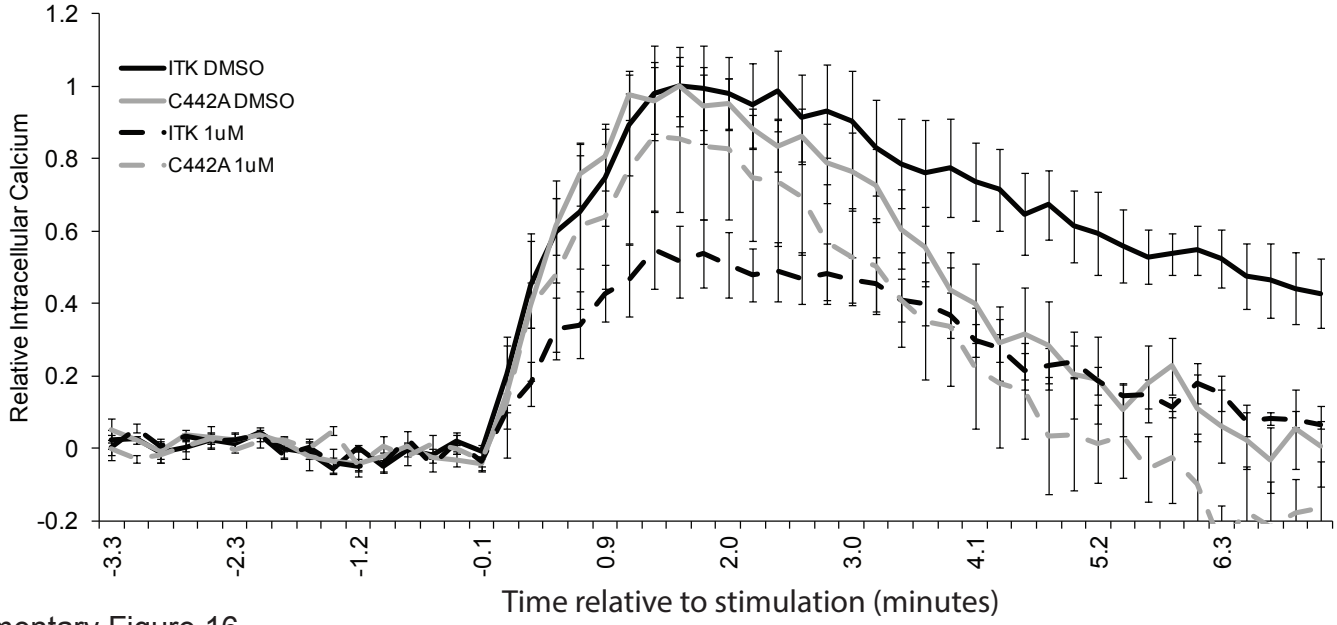

Supplementary Figure 16

Cell Line	GAPDH (Ct)	RLK (Ct)
Parental Jurkat	13.15	∞
Empty Vector	12.5	∞
RLK-Jurkat	12.7	24.6

Supplementary Figure 17

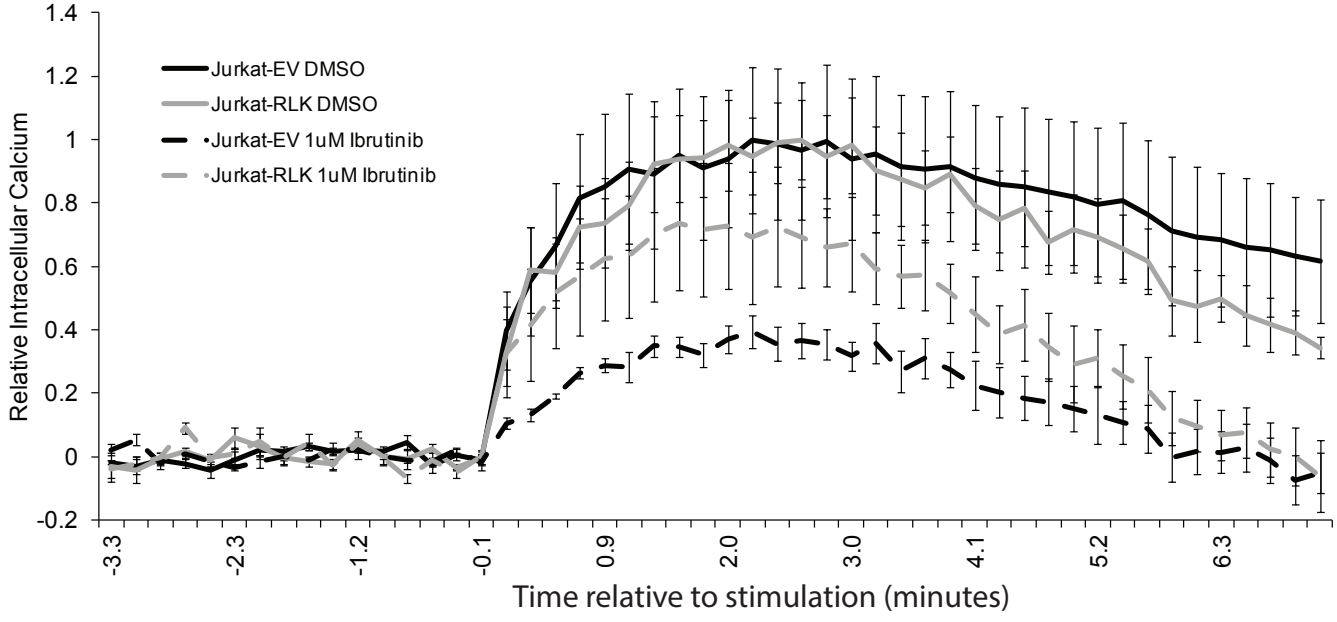

Supplementary Figure 18

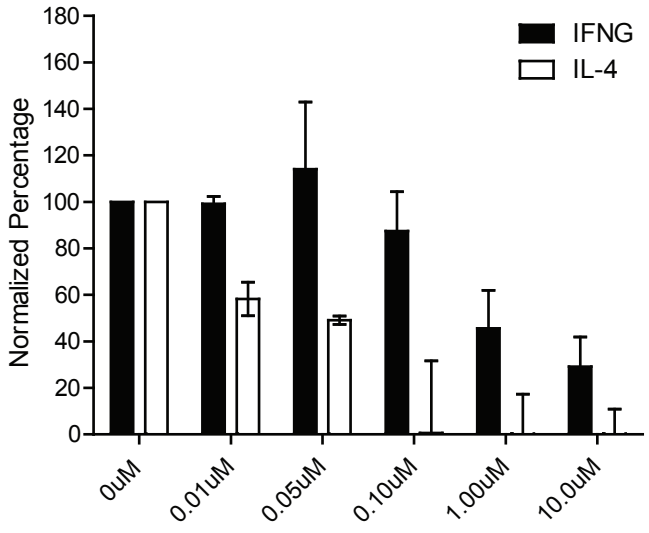

Supplementary Figure 19

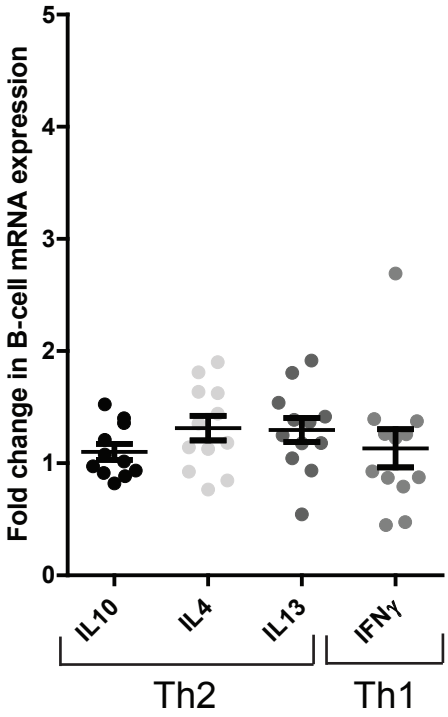

Supplementary Figure 20

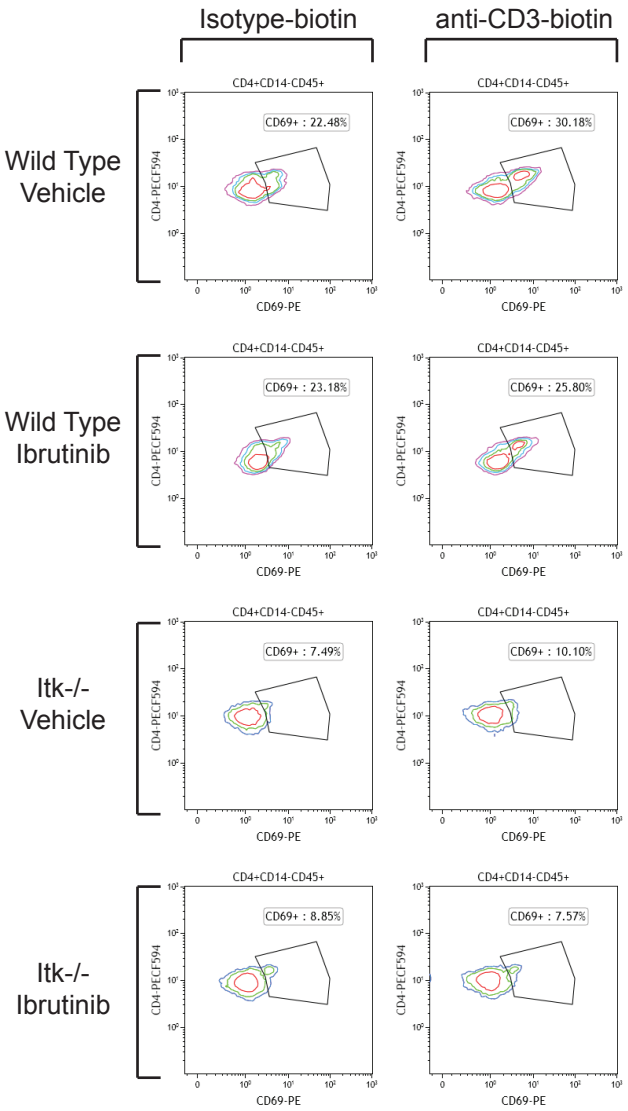

Supplementary Figure 21

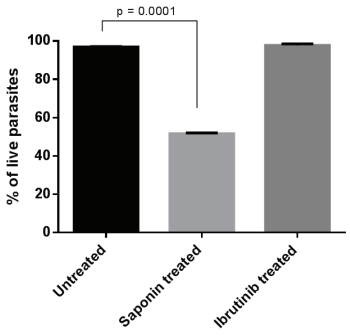

Supplementary Figure 22

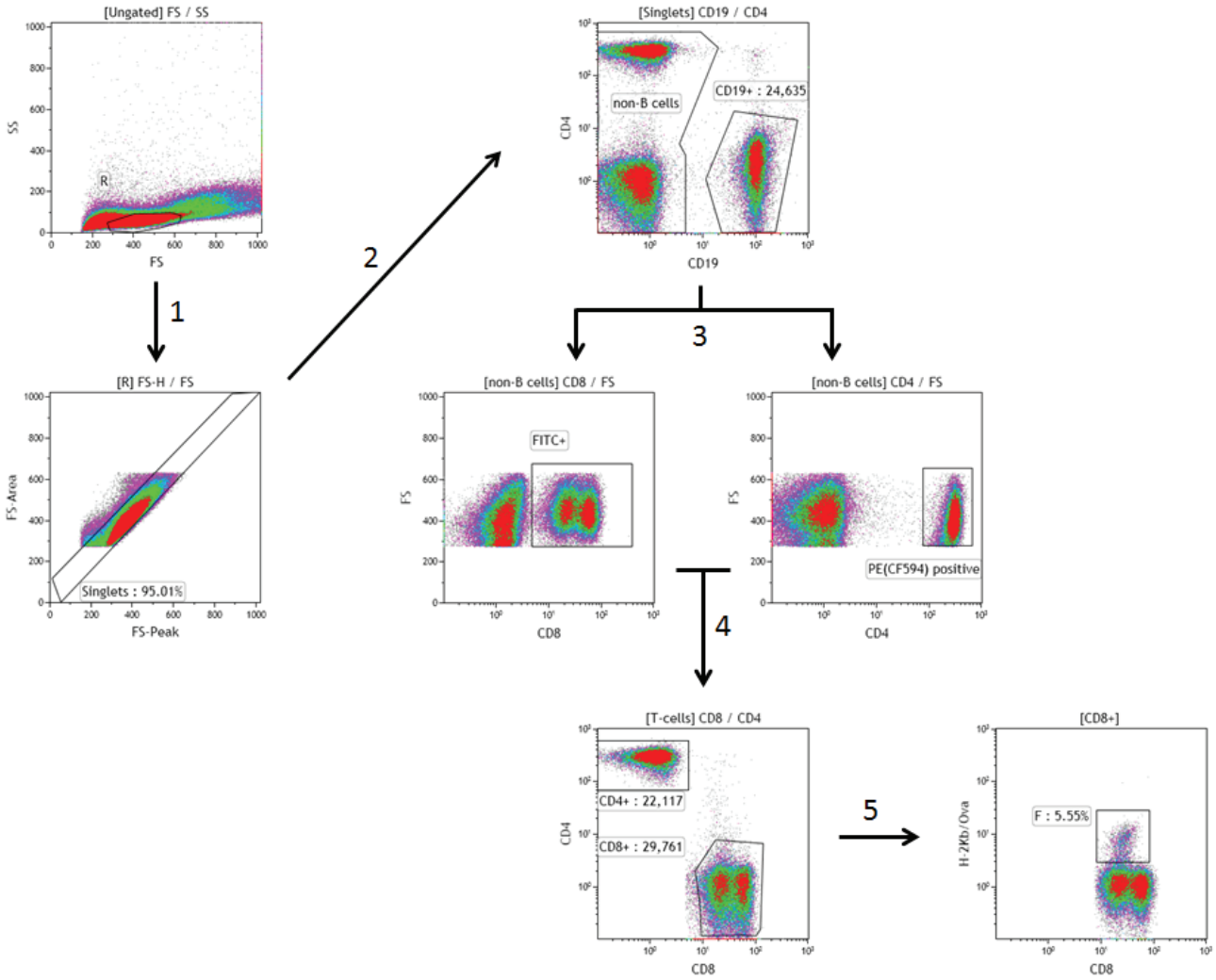

Supplementary Figure 23

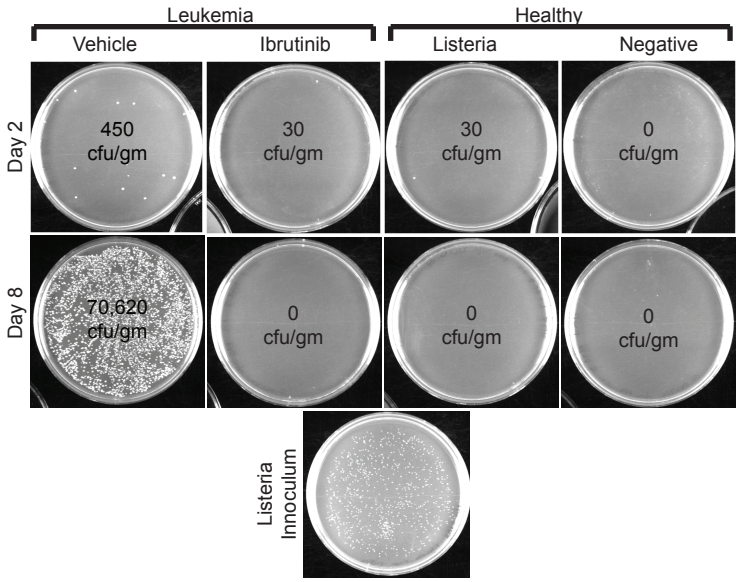

Supplementary Figure 24

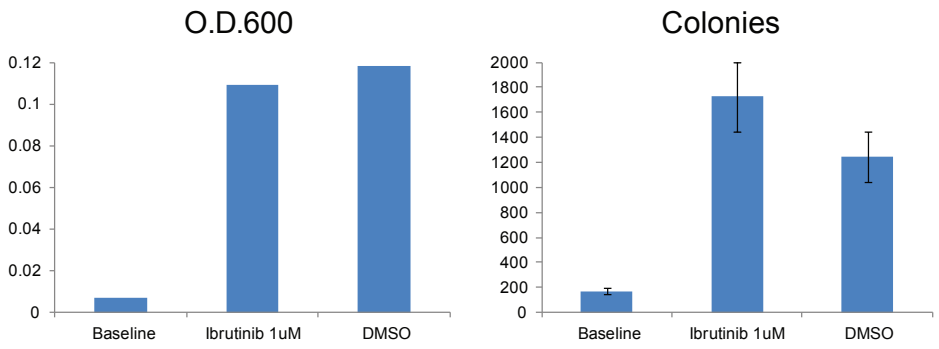

Supplementary Figure 25

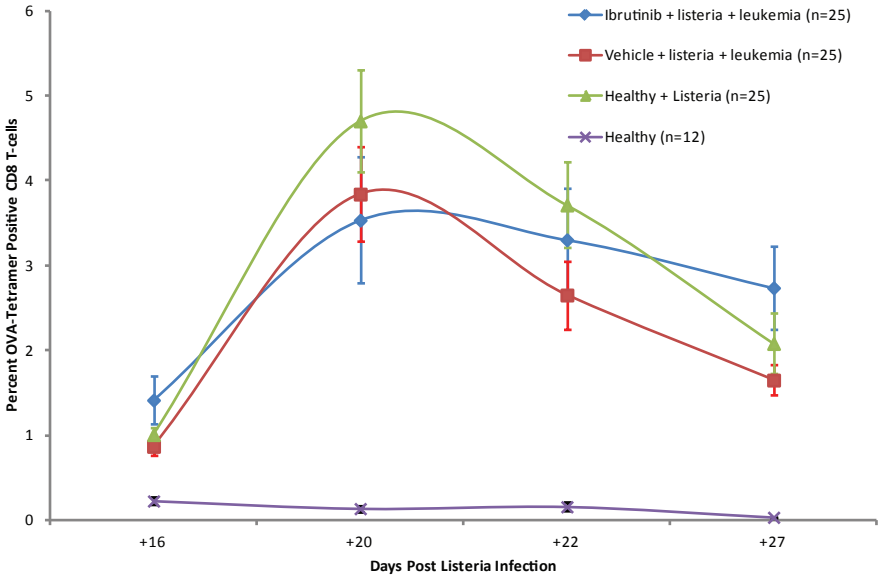

Supplementary Figure 26